

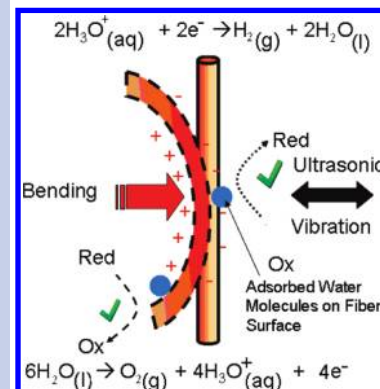
Direct Water Splitting Through Vibrating Piezoelectric Microfibers in Water

Kuang-Sheng Hong,[†] Huifang Xu,^{*,†} Hiromi Konishi,[†] and Xiaochun Li[‡]

[†]Department of Geoscience, and Materials Science Program and [‡]Department of Mechanical Engineering, and Materials Science Program, University of Wisconsin—Madison, 1215 W. Dayton Street, Madison, Wisconsin 53706

ABSTRACT We propose a mechanism, a piezoelectrochemical effect for the direct conversion of mechanical energy to chemical energy. This phenomenon is further applied for generating hydrogen and oxygen via direct water decomposition by means of as-synthesized piezoelectric ZnO microfibers and BaTiO₃ microdendrites. Fibers and dendrites are vibrated with ultrasonic waves leading to a strain-induced electric charge development on their surface. With sufficient electric potential, strained piezoelectric fibers (and dendrites) in water triggered the redox reaction of water to produce hydrogen and oxygen gases. ZnO fibers under ultrasonic vibrations showed a stoichiometric ratio of H₂/O₂ (2:1) initial gas production from pure water. This study provides a simple and cost-effective technology for direct water splitting that may generate hydrogen fuels by scavenging energy wastes such as noise or stray vibrations from the environment. This new discovery may have potential implications in solving the challenging energy and environmental issues that we are facing today and in the future.

SECTION Energy Conversion and Storage



Utilization of hydrogen energy has many attractive features, including energy renewability, flexibility, and zero green house gas emissions. In recent years, photocatalytic water splitting using oxide semiconductors under irradiation has received great attention.^{1–3} However, the number of available photocatalysts is currently limited, and their performance is hampered by their effectiveness, efficiency, and usage life. The demand for new mechanisms of direct water splitting to yield greater energy efficiency is rapidly increasing. In this study, we report the discovery of a phenomenon — the direct conversion of mechanical energy to chemical energy — termed the piezoelectrochemical (PZEC) effect. The mechanism of the water decomposition via the PZEC effect relies on the piezoelectric properties of the materials. Although the piezoelectric effect has been known for over 100 years and has been demonstrated in many fields,^{4,5} little work has been done to address its application in wet conditions (such as in solution) and particularly in the direct conversion of mechanical energy to chemical energy.

We report here the findings of our research on barium titanate (BaTiO₃) and zinc oxide (ZnO). Tetragonal BaTiO₃ and hexagonal ZnO with wurtzite structure display unique ferroelectric and piezoelectric properties.⁶ The crystals are commonly used in transducer and actuator devices.^{7,8} Recent study of ZnO nanowire arrays has indicated a direct conversion of mechanical to electrical energy by applying an oscillating force.^{9–11} Yet, few of the studies have demonstrated a direct conversion from mechanical energy to chemical energy in aqueous conditions. In this study, we use microfibers of ZnO and dendritic BaTiO₃ to initiate a phenomenon and drive

a nonspontaneous redox reaction, the formation of H₂ and O₂ gases from water, by using mechanical energy. Here, we show the capabilities of these materials for scavenging energy waste from the environment, such as noise and vibration, to generate hydrogen and oxygen gases.

SEM images of hydrothermally synthesized BaTiO₃ dendrites are shown in Figure 1a. Crystalline BaTiO₃ with perovskite structures were synthesized at 200 °C in an autoclave (see Experimental Methods for details). The crystalline BaTiO₃ exhibits a homogeneous dendritic morphology. The primary branches of the BaTiO₃ dendrite are typically ~10 μm long rods that grow along [001], while secondary branches develop along a different direction than the primary rod. The secondary branches are a few micrometers in length and have a similar width and height as the primary branches. Figure 1b is a transmission electron microscope (TEM) image of one synthesized BaTiO₃ dendrite. The inset electron diffraction pattern indicates that all of the branches in the dendrite have the same crystallographic orientation. Each dendrite is a single crystal of BaTiO₃. The high-resolution TEM (HRTEM) image (Figure 1c) shows (001) and (110) lattice fringes. Similarly, Figure 1d shows a SEM image of the as-synthesized ZnO fibers. From the figure, it is evident that the ZnO product consists mainly of straight, smooth, and crystalline microfibers. TEM images obtained for ZnO fibers grown on Si wafers are shown in Figure 1e. All fibers exhibit uniform

Received Date: January 11, 2010

Accepted Date: February 24, 2010

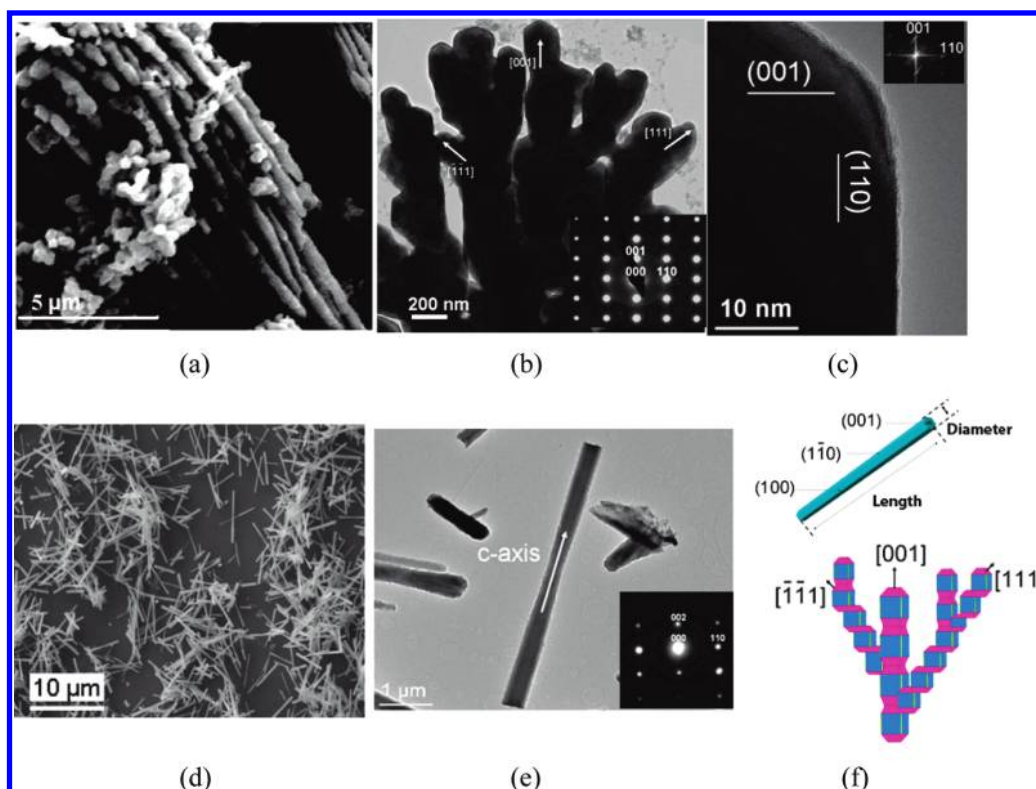


Figure 1. (a) SEM and (b) a typical TEM image of BaTiO₃ dendrites grown on a glass substrate; (c) HRTEM image of one BaTiO₃ crystal in the dendrite showing (001) and (110) lattice fringes. (d) SEM images and (e) TEM showing the typical morphology and crystal direction of ZnO fibers grown on a Si(100) wafer, in which the ZnO fibers were elongated along the *c*-axis with a diameter around 0.4 μm; (f) schematic diagrams showing shapes of a single ZnO fiber (upper) and BaTiO₃ dendrite (lower).

thickness and length. The fibers are ~0.4 μm in diameter, and the length ranges from 4 μm to greater than 10 μm. There is no secondary phase obtained in the interior of the grain or at the grain boundary. Each individual ZnO fiber is a single crystal growing along the [001] direction (see the inset electron diffraction pattern).

The performance of direct water splitting was further investigated, showing the capabilities of the ZnO fiber and BaTiO₃ dendrites for scavenging vibrational energy wastes from urban environments to generate hydrogen and oxygen gases from pure water. In order to first measure hydrogen gas production, ultrasonic wave vibrations using a Branson 5510-MT ultrasonic cleaner were applied to 5.0 mL of DI water in a Pyrex glass tube to determine the results of the piezoelectrochemical effect on as-synthesized ZnO fibers prepared on a Si(100) wafer of 1 × 1 cm². The results for hydrogen gas production are shown in Figure 2a. A control experiment was also conducted with a cleaned Si wafer (1 × 1 cm²), without ZnO fibers in the system. In the first period when external vibration was used (0–40 min), rapid hydrogen production was obtained at an initial rate of 3.4 × 10⁻³ ppm/s. The reaction cell was then evacuated at the 40th min, allowing a fresh run beginning at the 41st min. Ultrasonic wave vibration was turned off at the beginning of the 41st min, and the H₂ production was measured again. It was found that hydrogen generation stopped when the ultrasonic wave vibration was turned off, leading to a negligible H₂ production rate

(< 0.0001 ppm/s). This is similar to the control experiment (0–40 min). A possible reason for the low gas concentration in the experiments without ultrasonic vibration or the control experiment could be due to contamination from air in the room.

The oxygen production performance of ZnO fibers via the piezoelectrochemical effect was also investigated. Oxygen concentration was measured in solution as a function of time, as shown in Figure 2b. The response of the ZnO fibers to external vibrations was demonstrated by turning the ultrasonic wave in the system on and off. Consistent with the hydrogen production test, when ultrasonic waves were applied to ZnO fibers, the oxygen concentration grew rapidly at an initial rate of 1.7 × 10⁻³ ppm/s. Oxygen production stopped in the 41st–80th min, corresponding to when the ultrasonic waves were turned off. ZnO fibers in DI water with applied ultrasonic vibrations evolved hydrogen and oxygen gases with a stoichiometric equivalence of H₂/O₂ = 2:1. As with the previous experiments, no oxygen production was observed for the Si wafer control experiment.

Validation of the piezoelectrochemical effect was also demonstrated by applying ultrasonic vibrations to synthetic BaTiO₃ dendrites in pure water to generate H₂ gas. Figure 2c shows the evolution of H₂ from as-synthesized BaTiO₃ dendrites (dendrite mass = 7.5 × 10⁻³ g), with an average rate of H₂ evolution of approximately 1.25 × 10⁻² ppm/s in the first vibration event (0–50 min, Figure 2c). Gas generation

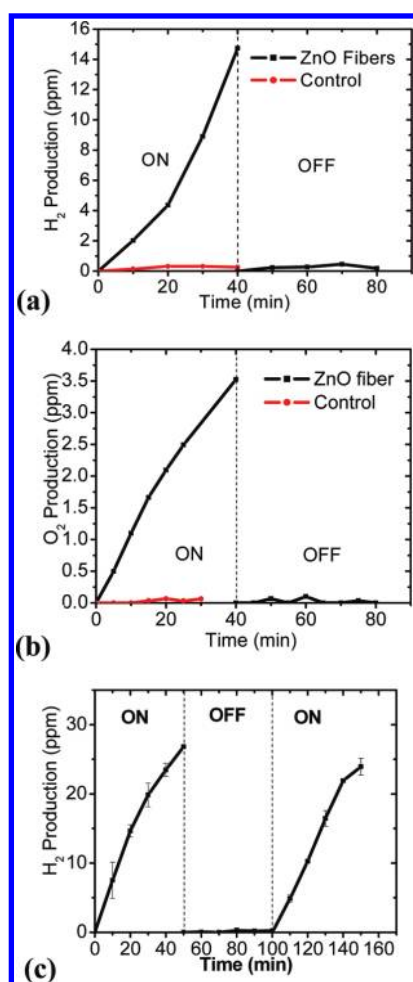


Figure 2. Evolution of (a) H₂ and (b) O₂ as a function of time, showing the performance of as-synthesized ZnO fibers on a Si(100) wafer ($1 \times 1 \text{ cm}^2$) in water responding to the ultrasonic waves; (c) H₂ evolution performance of as-synthesized BaTiO₃ dendrite with an effective mass of $7.5 \times 10^{-5} \text{ g}$ in the system.

stopped when the ultrasonic wave vibrations were turned off (51–100 min, Figure 2c). This shows that the reduction reaction of the water was induced by external mechanical energy and not by other forms of energy. BaTiO₃ will not react with water to generate hydrogen and oxygen without external stresses. After evacuating the reaction system and starting the ultrasonic waves again, a similar H₂ average production rate was obtained. A rate of nearly $9.13 \times 10^{-5} \text{ ppm/s}$ was obtained in the second period of vibration (101–150 min, Figure 2c). Results from both hydrogen and oxygen production tests using ZnO fibers and BaTiO₃ dendrites in water have successfully demonstrated the direct conversion of mechanical energy to the chemical energy via ultrasonic wave vibration. This energy production overcomes the standard oxidation–reduction potential of water for generating H₂ and O₂.

The physics and chemistry of generating hydrogen and oxygen gases from pure water arise from the combination of piezoelectric properties of ZnO fibers and BaTiO₃ dendrites and the redox reaction of water. Both ZnO and BaTiO₃ are

well-characterized piezoelectric materials. The piezoelectricity of each material arises from the lack of inversion symmetry in their crystal structures. Any deformation or strain acting on the material, such as the deformation of the Zn–O tetrahedra (Figure 3a) due to variation of the relative Ti–O positions (Figure 3b) will cause a nonzero dipole moment in the crystal lattice. Consequently, a strain-induced charge potential is produced on the surface of the material. Specific morphological aspects of ZnO and BaTiO₃ such as fibers and dendrites will acquire electric potentials on their surfaces if an external mechanical energy is applied that results in a bending (deformation) of the fibers or dendrites. The strain-induced electric potential formed on the fiber or dendritic surface in wet conditions (i.e., in pure water) is available for the reduction and oxidation reaction via charge transfer to species such as water molecules adsorbed on the surface (Figure 3c). Note that the developed potential must be greater than the standard redox potential of water (1.23 eV) to make electrons available to initiate the redox reaction in this experiment (Figure 3d). Residual charges or potentials lower than 1.23 eV will not participate in reactions to form H₂ and O₂ from water (Figure 3e).

Similarly, when the external mechanical input is turned off, electrical charges will no longer accumulate on the fiber surface. Thus, no sufficient potential can be used to reduce or oxidize the water molecules into hydrogen and oxygen, respectively. This is evidenced by the fact that we did not observe a rapid gas growth rate without vibration compared to the vibrational mode.

Note that the early proposed work of the mechanocatalytic effect using binary transition-metal oxides to split water was demonstrated based on the oxidation of metals as well as the reduction of the metal oxide in the reaction driven by mechanical energy forming H₂ and O₂.^{13,14} Although the works claimed a direct conversion from mechanical energy to chemical energy, the water decomposition mechanism was different from the piezoelectrochemical process. It was reported that metals formed during reaction are responsible for hydrogen production.¹⁵ In the PZEC effect, the catalyst (i.e., ZnO and BaTiO₃) participated in the direct water splitting reaction by donating strain-induced electrons and holes without been oxidized, reduced, or decomposed. Our TEM and XRD observations show that no metal species nor other extra phases appeared in our experiment samples before and after the reactions (see Supporting Information for XRD patterns). Our conclusions are that both ZnO fibers and BaTiO₃ dendrites show good responses to the application of ultrasonic vibrations by generating H₂ and O₂ directly from water. On the basis of the gas production tests above, we have confirmed the piezoelectrochemical effect by using the ZnO and BaTiO₃ fiber in wet conditions and not just the sample decomposition.

Figure 4a shows the H₂ evolution from pure water by as-synthesized ZnO fibers with different average fiber lengths (*L*) under ultrasonic wave vibration. The PZEC efficiency due to different average fiber lengths is shown in Figure 4b. The observed chemical energy output by a single ZnO fiber with $L = 5.7 \mu\text{m}$ in one vibration event was $\sim 1.6 \times 10^{-16} \text{ J}$, and the effective mechanical energy input applied on the fiber was $\sim 2.3 \times 10^{-15} \text{ J}$ (see Supporting Information for detailed

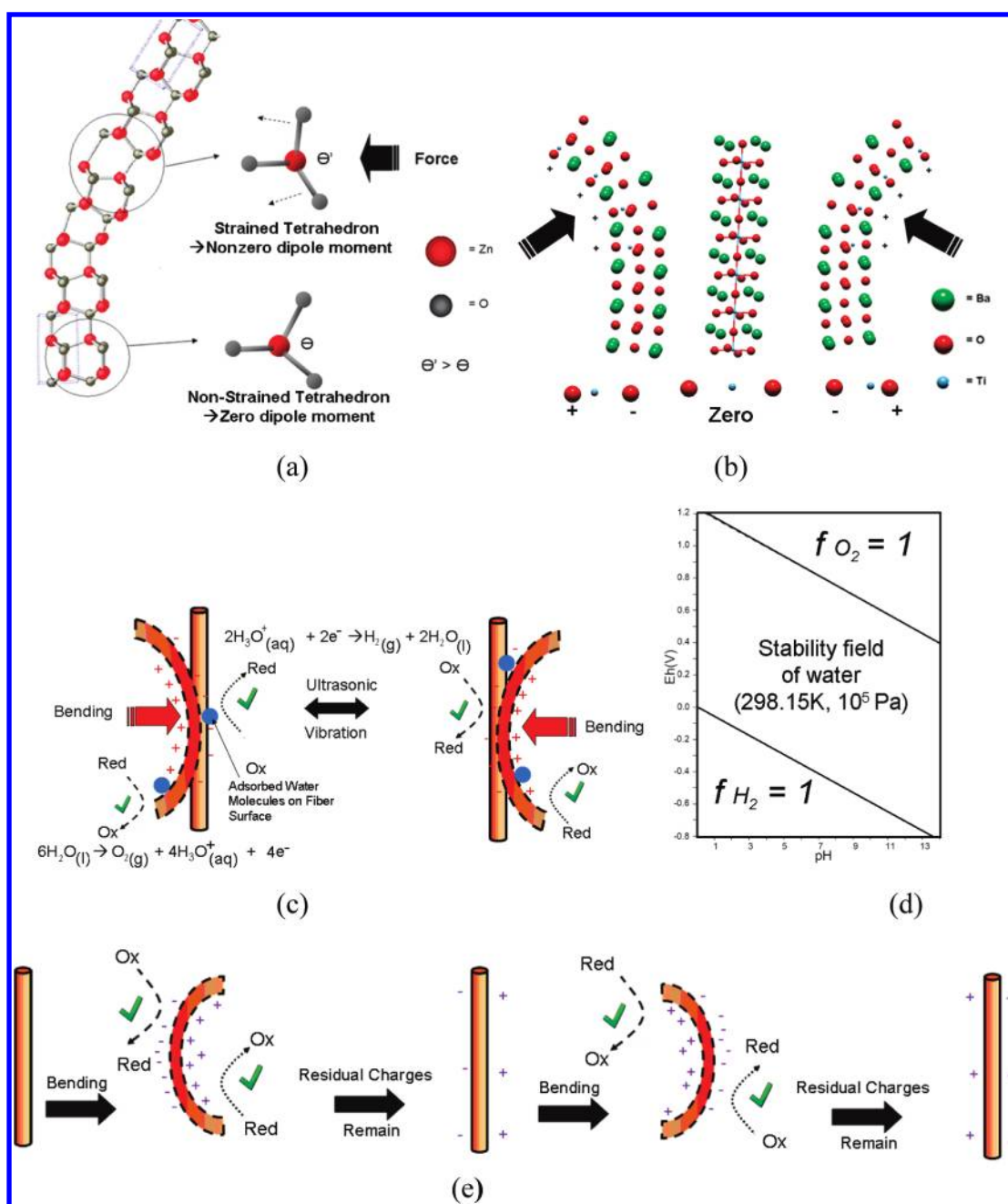


Figure 3. Schematic diagrams showing the charges developed on (a) a ZnO fiber surface through bending with ultrasonic vibration. When deformed, the Zn–O tetrahedron changes its relative position, leading to a nonzero dipole moment. (b) By the same analogy, the charge development on the elongated BaTiO₃ microcrystals is due to its piezoelectric property in which the Ti–O distance changes under bending. (c) H₂ and O₂ are produced by deforming a ZnO fiber or BaTiO₃ dendrite in water via oxidation–reduction reactions. (d) Eh–pH diagram showing the stability field of water. Two heavy lines indicate a condition with 1 atm of pressure of hydrogen and oxygen gases, which shows that the required potential for water decomposition at standard condition is 1.23 V.¹² (e) Procedures of piezoelectrochemical reactions through fiber bending, showing that only the induced potential greater than that of standard reduction potential of water will trigger the reaction.

calculations). The PZEC mechanical to chemical efficiency was found to be ~6.9%. Increasing the ZnO fiber length to $L = 7.8 \mu\text{m}$ increased reaction efficiency to ~18%. An increase in the efficiency can be explained by the strain-induced voltage related to the curvature of the fiber. Fibers with greater lengths (L) exhibit a greater bending curvature than that of shorter fiber lengths when under the same applied force in a

vibration event.¹¹ Due to this property, in our ZnO fiber trials with equal mechanical vibration, longer fibers built up a higher number of voltages that exceed the water reduction potential. Therefore, the trials with a longer fiber length demonstrated an increased hydrogen production performance, providing higher efficiency for mechanical to chemical energy conversion.

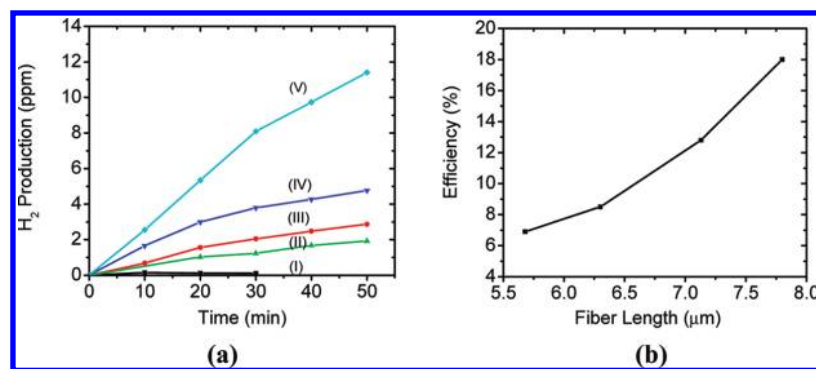


Figure 4. (a) Hydrogen evolution of the ZnO fibers under standard condition with various average fiber lengths: (I) control or no fiber, (II) 5.7 μm , (III) 6.3 μm , (IV) 7.3 μm , and (V) 7.8 μm . (b) Efficiency of the piezoelectrochemical effect for converting mechanical energy into chemical energy as a function of ZnO fiber length.

The PZEC efficiency of BaTiO₃ dendrites in water was also demonstrated through our experiments. Here, the H₂ production test obtained a production rate of 1.25×10^{-2} ppm/s. In addition, on the basis of SEM images, the density (6.08 g/cm³) and the volume of a single BaTiO₃ dendrite branch, the overall BaTiO₃ dendrites mass (7.5×10^{-3} g), and the estimated number of the dendrites in the system, the mechanical to chemical conversion efficiency of the BaTiO₃ dendrites with an average length of 10 μm was found to be 3.2%. BaTiO₃ dendrites intrinsically have a slightly greater electromechanical coupling coefficient value (k) ($k_{33, \text{BaTiO}_3} = 0.49$; $k_{33, \text{ZnO}} = 0.408$) and, extrinsically, a larger aspect ratio than that of ZnO fibers. This indicates a higher efficiency from the BaTiO₃ dendrites expected. However, BaTiO₃ dendrites are composed of branch-like structures which may limit the degree of deflections of each individual BaTiO₃ branch with applied vibrations. Unlike ZnO fibers, which spread freely through a given space, BaTiO₃ dendrites are bundled together in groups. As a result, the dendrites are more likely to be in contact with each other when deformation occurs, leading to partial charge cancellations and a lower gas production rate from the reaction. Morphologically, we anticipate that performance will be greatly increased by selecting chemically stable fiber and dendrite materials with greater k values, a larger aspect ratio, and surface areas and ensuring that the fiber and dendrites are spaced out for more bending space to avoid charge cancellations.

Using fibrous ZnO and dendritic BaTiO₃ catalysts with piezoelectric properties, we have demonstrated the PZEC effect for generating H₂ and O₂ from water. We have successfully verified a direct conversion of mechanical energy to chemical energy. Finding an optimum fiber length and introducing the resonance frequency of ZnO and BaTiO₃ for the direct water splitting process, it may be possible to obtain a much greater H₂ and O₂ production rate. Utilizing the piezoelectric fibrous samples, the phenomena demonstrated could usher in a new era in the field of recycling environmental energy wastes. Vibrational energy waste generated in the environment from noise, wind power, running water, or water wave action can be scavenged or harvested as a driving force for direct water splitting, thereby forming H₂ and O₂ by means of PZEC fiber arrays implanted on a substrate. The fiber arrays can also be used to harvest artificial energy wastes

such as traffic noise and vibrations and convert them into hydrogen and other chemical energies. The principle of the PZEC effect using these fibers could be a very important step forward in nanotechnology that recycles the energy wastes from the environment into precious alternative chemical energy. This work will open a new field of study on hydrogen generation, redox reactions, and energy recycling.

EXPERIMENTAL METHODS

The BaTiO₃ dendrite samples of the PZEC catalyst were synthesized by a hydrothermal method.¹⁵ All of the chemicals that were used as starting materials had a purity of 99.99%. The precursor Ti(OH)₄ was prepared by adding 25 mL of Ti(OC₂H₅)₄ dropwise into 1.0 M acetic acid. The solution was settled, allowing the precipitate to form in 72 h, and followed by rinsing of the product with DI water and drying at 60 °C. The as-synthesized Ti(OH)₄ precursor and commercially available Ba(OH)₂·8H₂O were then added (Ti/Ba = 1:1 in molar ratio) into 0.25 M NaOH. After that, the mixture in a Teflon cup with 60% capacity was stirred and sealed tightly in a stainless steel autoclave. The closed bomb (Parr-type) was maintained at 200 °C for 68 h for hydrothermal reaction. The bomb was then cooled naturally to room temperature. The resulting white precipitate was washed extensively with DI water to remove any adsorbed impurities and finally dried at room temperature.

A hydrothermal method was used to synthesize ZnO fibers.¹⁶ Hexamethylenetetramine (C₆H₁₂N₄) and zinc nitrate hexahydrate (Zn(NO₃)₂·6H₂O) precursor solutions were mixed together (1:1 molar ratio) in a Teflon cup with 60% capacity followed by magnetic stirring for 15 min. The mixture was then sealed tightly in a stainless steel autoclave. The closed bomb was heated at 95 °C for 48 h. After that, the bomb was cooled naturally to room temperature. The final products were washed with DI water and dried at room temperature.

Dried samples were characterized by using powder X-ray diffraction using a Scintag Pad V diffractometer system with a Cu K α beam ($\lambda = 0.1541$ nm). Morphological observation and electron diffractions (ED) on particles were confirmed on a Philips CM 200UT transmission electron microscope (TEM) with a spherical aberration coefficient (C_s) of 0.5 mm and a

point-to-point resolution of 0.19 nm. The TEM was operated at an accelerating voltage of 200 kV. Scanning electron microscopy (SEM) was also conducted with a Hitachi S-3400N variable pressure microscope with a tungsten filament that delivers at least 50 nA of beam current. The experiment of water splitting to hydrogen and oxygen was carried out using a sealed glass tube and samples in water under a standard condition. Glass tubes, 0.5 in. in diameter and 1 ft in length, were used for the experiment. The reaction cell (glass tube) was filled with nitrogen gas after adding the samples. To monitor the hydrogen concentration variation, the gas inside of the cell was extracted by syringe and injected into an external hydrogen analyzer. The amount of hydrogen gas (H₂) produced from the water splitting experiment was monitored using an AMETEC Trace Analytical ta3000 gas chromatograph equipped with a reduction gas detector (RGD) sensor for hydrogen detection. Nitrogen gas (N₂) of 99.998% purity at a flow rate of 20 cc/min was applied as the carrier gas. The detection limit of the H₂ analyzer was 10 ppb hydrogen. To monitor the amount of oxygen produced from the system, the oxygen concentration in solution was monitored as a function of time by using an isolated dissolved oxygen meter ISO₂ equipped with an OXELP probe (World Precisions Instruments).

SUPPORTING INFORMATION AVAILABLE Additional materials about catalyst characterization and efficiency calculation. This material is available free of charge via the Internet at <http://pubs.acs.org>.

AUTHOR INFORMATION

Corresponding Author:

*To whom correspondence should be addressed. Tel: 608-265-5887. E-mail: hfxu@geology.wisc.edu.

ACKNOWLEDGMENT The authors acknowledge support from the NASA Astrobiology Institute (N07-5489), the National Science Foundation (EAR-0810150), U.S. Department of Energy, the Graduate School of the University of Wisconsin, and Alumni of the Department of Geoscience. We thank Prof. Eric Roden for the H₂ and O₂ analyzer instruments. H.X. conceived the idea and contributed to manuscript writing. K.S.H. performed most of the experiments and drafted the manuscript. H.K. performed the TEM and analysis and the ZnO fiber/BaTiO₃ dendrite orientation. K.S.H., H.X., and X.L. planned the research and analyzed and interpreted the data.

REFERENCES

- Anpo, M. Preparation, Characterization, and Reactivities of Highly Functional Titanium Oxide-Based Photocatalysts Able to Operate under UV-visible Light Irradiation: Approaches in Realizing High Efficiency in the Use of Visible Light. *Bull. Chem. Soc. Jpn.* **2004**, *77*, 1427–1442.
- Kudo, A.; Miseki, Y. Heterogeneous Photocatalyst Materials for Water Splitting. *Chem. Soc. Rev.* **2009**, *38*, 253–278.
- Maeda, K.; Teramura, K.; Lu, D.; Takata, T.; Saito, N.; Inoue, Y.; Domen, K. Photocatalyst Releasing Hydrogen from Water. *Nature* **2006**, *440*, 295.
- Uchino, K. *Piezoelectric Actuators and Ultrasonic Motors*; Kluwer Academic Publishers: London, 1997.
- Herbert, J. M. *Ferroelectric Transducers and Sensors*; Gordon and Breach: London, 1982.
- Oren, E. E.; Tas, A. C. Hydrothermal Synthesis of Dye-Doped BaTiO₃ Powders. *Metall. Mater. Trans. B* **1999**, *30*, 1089–1093.
- Look, D. C. Recent Advances in ZnO Materials and Devices. *Mater. Sci. Eng., B* **2001**, *80*, 383–387.
- Cao, H.; Xu, J. Y.; Zhang, D. Z.; Chang, S. H.; T., H. S.; Seeling, E. W.; Liu, X.; Chang, R. P. H. Spatial Confinement of Laser Light in Active Random Media. *Phys. Rev. Lett.* **2000**, *84*, 5584–5587.
- Wang, Z. L. Piezoelectric Nanogenerators Based on Zinc Oxide Nanowire Arrays. *Science* **2006**, *312*, 242–246.
- Wang, X. D.; Zhou, J. J.; Song, H.; Liu, J.; Xu, N. S.; Wang, Z. L. Piezoelectric Field Effect Transistor and Nanoforce Sensor Based on a Single ZnO Nanowire. *Nano Lett.* **2006**, *6*, 2768–2772.
- Song, J. H.; Zhou, J.; Wang, Z. L. Piezoelectric and Semiconducting Coupled Power Generating Process of a Single ZnO Belt/Wire. A Technology for Harvesting Electricity from the Environment. *Nano Lett.* **2006**, *6*, 1656–1662.
- Takeno, N. *Atlas of Eh-pH Diagrams, Intercomparison of Thermodynamic Databases*. National Institute of Advanced Industrial Science and Technology: Tokyo, 2005.
- Hara, M. K.; Hasei, H.; Yashima, M.; Ikeda, S.; Takata, T.; Kondo, J. N.; Domen, K. A Study of Mechano-Catalysts for Overall Water Splitting. *J. Phys. Chem. B* **2000**, *104*, 780–785.
- Ikeda, S.; Takata, T.; Kondo, T.; Hitoki, G.; Hara, M.; Kondo, J. N.; Domen, K.; Hosono, H. Mechano-Catalytic Overall Water Splitting. *Chem. Commun.* **1998**, 2185–2186.
- Wang, Y.; Xu, G.; Yang, L.; Ren, Z.; Wei, X.; Weng, W.; Du, P.; Sheng, G.; Han, G. Hydrothermal Synthesis of Single-Crystal BaTiO₃ Dendrites. *Mater. Lett.* **2009**, *63*, 239–241.
- Li, D.; Liu, Z. T.; Leung, Y. H.; Durisic, A. B.; Xie, M. H.; Chan, W. K. Transition-Metal-Doped ZnO Nanorods Synthesized by Chemical Methods. *J. Phys. Chem. Solids* **2008**, *69*, 616–619.